

Implementation of Resistance Training Using an Upper-Limb Exoskeleton Rehabilitation Device for Elbow Joint

Zhibin Song^{1,*} Shuxiang Guo^{1,2} Muye Pang³ Songyuan Zhang³ Nan Xiao¹
Baofeng Gao¹ Liwei Shi¹

¹Department of Intelligent Mechanical Systems Engineering, Kagawa University, Hayashi-cho, Takamatsu 761-0396, Japan

²Automation College, Harbin Engineering University, Harbin 150001, China

³Graduate School of Engineering, Kagawa University, Takamatsu 760-8521, Japan

Received 9 Oct 2012; Accepted 19 Feb 2013; doi: 10.5405/jmbe.1337

Abstract

Most exoskeleton devices for upper-limb rehabilitation are heavy and bulky. The present study develops a light and wearable exoskeleton device for passive and resistance training that can potentially be used in home rehabilitation. A method for implementing resistance rehabilitation based on the proposed upper-limb exoskeleton rehabilitation device is proposed. The method is able to be used commonly in the field of Human-machine force interaction where the machine is of high friction, non-backdrivability which causes the difficulty to obtain contact force. To verify the efficacy of the method, experiments were conducted under two conditions, namely with passive degrees of freedom unlocked and locked, during elbow flexion and extension. In each case, three levels of resistance were generated and provided to the user. The processed EMG signals can be used to verify that the method is effective in both of cases.

Keywords: Resistance training, Surface electromyography (sEMG), Upper-limb exoskeleton rehabilitation device (ULERD), Impedance

1. Introduction

Stroke is a leading cause of disability in the United States, affecting an estimated 6.4 million Americans [1]. Traditional rehabilitative therapies help regain motor function and ameliorate impairment [2], but they depend on the therapist's experience and require many therapists, which is cost-prohibitive. Some rehabilitation robots have been developed to help stroke survivors recover motor function [3-6]. Robots used for upper-limb rehabilitation can be divided into exoskeleton and end-effector types [7,8]. However, most existing rehabilitation robots are heavy and large and thus unsuitable for home rehabilitation. In this study, a light and wearable exoskeleton device is designed and developed for home rehabilitation.

Upper-limb rehabilitation robots are typical human-machine interaction (HMI) devices. However, they are different from other HMI devices because they should be able to execute training strategies in clinic regardless that they are end effector type or exoskeleton type according to evidence-based medicine. According to the statement in some literature

[9-12], physical rehabilitation training strategies can be mainly classified as passive, resistance [13], and bilateral rehabilitation [14,15]. Rehabilitation robots also adjust the training level of a given strategy according to individual impairments. Patients can generally perform passive rehabilitation reasonably well following a weak stroke, and survivors of a mild stroke get good benefits from resistance rehabilitation. Hemi-paralyzed patients tend to perform bilateral rehabilitation. Our previous study discussed the implementation of passive rehabilitation and bilateral rehabilitation using an upper-limb exoskeleton rehabilitation device (ULERD) and some preliminary research has been performed for resistance rehabilitation focusing on the elbow joint [16]. The present study proposes an implementation method for resistance rehabilitation suitable for a ULERD. Since obtaining the contact force between the user and the device is difficult using a sensor while a portable exoskeleton device is being worn, surface electromyography (sEMG) signals were acquired and analyzed to evaluate the resistance rehabilitation performed by unimpaired subjects.

Two fundamental control methods are categorized according to inputs and outputs of system to implement resistance rehabilitation strategy using an electromechanical system [17]. One is impedance control, in which the motion input by the user is measured and the force is fed back to the user. The other is admittance control, in which forces exerted by a user are measured and the device reacts with proper

* Corresponding author: Zhibin Song
Tel: +81-087-8642356; Fax: +81-087-8642369
E-mail: songbin02717@hotmail.com

displacement. The paradigm for impedance control is motion in and force out; the paradigm for admittance control is force in and motion out. Both methods were developed to implement the same goal, which was to provide virtual resistance to humans using an electromechanical device; however, they adapt different approaches because of their different application condition.

Impedance control, used commonly in commercial haptic devices (e.g. Phantom Omni), requires a low-inertia, low-friction, and highly backdrivable device. However, its performance is lacking in the region of higher forces, high mass, and high stiffness, and adding complex end effectors is difficult [17,18]. In contrast, admittance control devices allow considerable freedom in the mechanical design of the device because backlash and tip inertia can be eliminated. Admittance control can be adopted when the contact force between the human and the device can be detected accurately. A ULERD adopts a high-ratio gearhead, so it is not backdrivable. It has multiple degrees of freedom (DoFs) to assist or resist multiple motions of the upper limbs with mounts on the upper limbs, so an accurate contact force between the human and the device cannot be obtained easily using force sensors. Therefore, these two methods are not suitable for ULERDs. Different from tactility or resistance exerted on the human by the deformation of a haptic device via impedance control, deformation of human skin and muscle induces resistance on the human body, which is difficult to model. Therefore, in this study, a method is proposed to detect the motion of human upper limbs related to the ULERD by creating an elastic contact condition between them, which can be considered an elastic extension of human muscles. A similar method is adopted in serial elastic actuators, which provide linear motion detection using serial elastic springs [19]. The present study focuses on generating resistance to the human forearm during elbow flexion and extension by detecting rotating motion of the forearm. Experiments were carried out with three healthy subjects to demonstrate the features of the proposed system. Testing with actual patients in a medical center is being planned. The experiments included two main cases: generating three levels of resistance with passive DoFs locked and unlocked, respectively, in the elbow joint. The experimental efficacy was evaluated by detecting and processing sEMG signals from the biceps and triceps muscles, which indicate whether the subjects perform the motion against the resistance derived from the device. This project was approved by the institutional review board of Kagawa University, Japan.

2. Overview of ULERD development

2.1 Theory of human limb physical rehabilitation

The design and development of a rehabilitation robot should include training strategies based on neurorehabilitation theory to achieve the rehabilitation of patients with motor-function impairment. Passive, resistance, and bilateral training are three strategies for physical rehabilitation of the upper limbs [14,15,20]. Some combinations of these strategies have also been used [14,15].

Passive training is performed by patients who have no muscle strength. It assists them to perform some tasks with a therapist or a rehabilitation device. It is usually suitable for patients with severe impairments and very limited motor function. Resistance training is performed by patients who have some muscle strength with a therapist or a rehabilitation device. It is usually suitable for weak patients with limited motor function. Bilateral training requires the patient to perform symmetrical or coordinative motion with bilateral limbs, which has been demonstrated to be effective [21]. It is usually performed by hemiplegic patients and commonly requires a rehabilitation device. The present study focuses on implementing resistance training using a ULERD to generate resistance during elbow flexion and extension.

2.2 System description

The proposed system for upper-limb resistance training includes a human machine interface HMI and a robot manipulator (ULERD). The predefined task is shown on a computer screen using a graphical user interface (GUI). The developed GUI guides a user to effectively perform the tasks. An inertia sensor mounted on the user's wrist is used to detect motion of the forearm, and the values derived from the inertia sensor are used to generate the different impedance combined with different models. sEMG signals from the biceps and triceps muscles were used to evaluate the proposed method.

2.3 ULERD design

The motivation for the ULERD design was to provide passive and resistance training for patients with motor dysfunction to recover upper-limb motor function especially in the elbow and wrist joints. The goal was to make the device wearable and portable for home rehabilitation. The basic design structure of the ULERD is depicted in Fig. 1. Three active DoFs were designed for the elbow and wrist, namely elbow flexion/extension (F/E), forearm pronation/supination (P/S), and wrist flexion/extension (F/E). These three DoFs are both actuated and sensorized. Four passive DoFs were added, consisting of two DoFs (one for rotation and the other for translation) in the elbow joint and the other two (one for rotation and the other for translation) in the wrist joint after considering many factors, such as variation in the flexion/

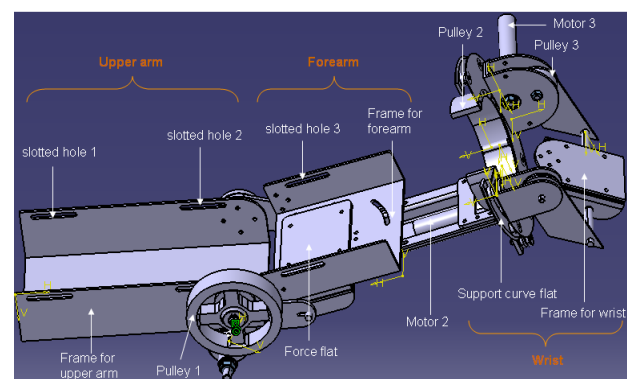


Figure 1. Top view of ULERD. The device includes three DC motors that provide elbow flexion/extension, wrist pronation/supination, and wrist flexion/extension, respectively.

extension axis [22], individual variation in the physical dimensions of the joint, and correlation between the wrist and elbow joint during elbow flexion and extension. The two passive rotational DoFs were sensorized with potentiometers, and can be turned on or off depending on requirements.

To reduce the mass of the device, high-power-density brushless DC motors are used and the main frame of the device is aluminum. The total weight of its body is 1.3 kg. Table 1 shows the continuous maximum torque and workspace of each joint. The upper limb was fixed to the device using several elastic belts passing through slotted holes on the upper arm and forearm of the ULERD. The palm can also be fixed to the wrist part of the ULERD using an elastic belt. The ULERD was designed to allow users to put it on conveniently by themselves. The distance between the elbow joint and the wrist part and the angle between the upper arm and forearm part of the ULERD can be moderately adjusted to fit the user. Figure 2 shows a user wearing the ULERD.

Table 1. Specifications for each joint.

	Continuous maximum torque (Nm)	Device joint workspace (deg)
Elbow F/E	15	180/0
Forearm P/S	9	85/75
Wrist F/E	7	70/65

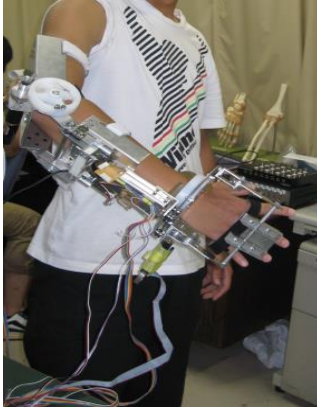


Figure 2. User wearing ULERD on his upper limb.

2.4 Kinematics of ULERD elbow joint

In this paper, the implementation of resistance training using the ULERD focused on the elbow joint, whose kinematics are discussed below. The passive DoFs in the elbow joint (one translation and one rotation) were designed to make the device compliant with the user's elbow flexion and extension. These DOFs can be locked via two bolts. Passive DoFs also compensates for faulty rotation of human joints. However, this is not ideal for some patients. For example, the gravity force on the forearm and wrist parts of the ULERD cannot be compensated for completely, so the device must be supported by the human forearm to some degree during resistance training. Considering that patients who actively train have a certain ability to move their upper limbs, the passive DoFs are locked during resistance training, which enhances the resistance efficacy and improves the resistance rehabilitation effect. Experiments were conducted to show the effect of resistance training with and without passive DoFs. The typical

integration structure of passive and active DoFs in the elbow joint is analyzed in detail in the following section.

Figure 3 shows a schematic model of the ULERD elbow joint with passive DoFs. In this figure, a rotational DoF located at O_1 is actuated, and two passive DoFs (rotational and translational) are located at point A. It is supposed that the upper arm is fixed in the y axis. O_1 is the rotational center of the active DoFs, O_2 is the rotational center of the user's elbow joint, and the forearm is fixed on component AB. In this figure, a crank and rocker mechanism is formed where point O_1 does not overlap O_2 . CD is the center disparity of the elbow joint axis on the sagittal plane during elbow flexion and extension. From Fig. 3, the basic relationships between the device and the human elbow joint are obtained as:

$$\vec{l}_{O_1A} + \vec{l}_{AO_2} = \vec{l}_{O_1O_2} \quad (2)$$

$$\psi_1 = \psi_2 + \psi_3 \quad (3)$$

where ψ_1 is the angle from AO_1 to the x axis; ψ_2 is the angle from AO_2 to the x axis, which can be obtained from the inertia sensor; and ψ_3 is the angle from AO_2 to AO_1 (its detection method is presented below). Equation 2 can be rewritten as a complex function as:

$$l_{O_1A} \exp(i\psi_1) + l_{AO_2} \exp(i\psi_2) = x + yi \quad (4)$$

Then:

$$l_{O_1A} \cos \psi_1 + l_{AO_2} \cos \psi_2 = x \quad (5)$$

$$l_{O_1A} \sin \psi_1 + l_{AO_2} \sin \psi_2 = y \quad (6)$$

It is supposed that at any moment, the elbow joint axis is constant, so the differential of Eq. (4) is:

$$l_{O_1A} \omega_1 i \exp(i\psi_1) + V_{O_1AO_2} \exp(i\psi_1) + l_{AO_2} \omega_2 \exp(i\psi_2) = 0 \quad (7)$$

where $V_{O_1AO_2}$ is the velocity of AB along AO_1 and can be obtained as shown below. Equation (6) is multiplied by $\exp(-i\psi_1)$.

$$l_{O_1A} \omega_1 i + V_{O_1AO_2} + l_{AO_2} \omega_2 \exp(i\psi_2 - i\psi_1) = 0 \quad (8)$$

$$l_{O_1A} \omega_1 = l_{AO_2} \omega_2 \cos(\psi_2 - \psi_1) \quad (9)$$

$$V_{O_1AO_2} = l_{AO_2} \omega_2 \sin(\psi_2 - \psi_1) \quad (10)$$

The position of the elbow joint axis can be calculated using Eqs. (5-10).

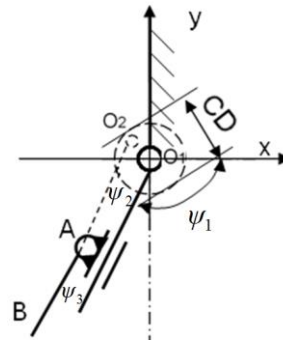


Figure 3. Schematic structure of ULERD elbow joint.

3. Control methodology

According to the literature [17,18], two main control methods are widely used in HMI systems to generate a force interaction, namely impedance and admittance control. The main difference between them is the application condition. Impedance control requires high backdrivability and low inertia and mass. An impedance control device should allow free movement in response to the operator's motion commands, such that no resistance to motion occurs when the user manipulates the device in free space. Furthermore, low inertia and friction improve device transparency. A typical application is the Phantom family (Sensable Technologies, Woburn, MA, USA). Alternatively, admittance control can be used in a high-inertia system but requires a highly accurate contact force between the human and machine. The machine is controlled based on the virtual environment model.

These methods have the same objective of implementing a compliant interaction between the human and machine but adapt different approaches. In the ULERD, the high-ratio gearhead results in no backdrivability, but it covers human limbs closely, which results in difficulties obtaining an accurate contact force. A similar circumstance has been previously reported [23], in which the exoskeleton device can follow human motion by forcing the motor to rotate over low angles, which are detected by hall sensors. Human motion can be tracked but the transparency of the system is low. In this study, elastic components were used to detect human motion in the HMI system in which the device has no backdrivability. Similar components were proposed and used in a serial elastic actuator [24], in which linear elastic springs were used to detect the motion of the load. In this study, elastic materials were used to detect the relative rotation of the user's forearm with respect to the upper arm. Based on the proposed methods, variable resistance can be provided to the user's upper forearm, such as a spring model, damper model, or integration model, and even water resistance. Experiments conducted using the proposed method focused on the elbow joint.

The control system scheme is shown in Fig. 4. Human limb motion information, namely position, velocity, and acceleration, was obtained from an inertia sensor. These parameters were calculated based on the motion of the virtual model and then sent to the motor controllers as input. Because the proposed method mainly uses the relative displacement between the human limb and the device, the motors were driven into position with closed-loop velocity control and an inertia sensor and encoders using a proportional-integral-derivative (PID) control algorithm. To evaluate the performance of the proposed method, sEMG signals from the biceps and triceps muscles were recorded during elbow flexion and extension.

Figure 5 shows a schematic model of resistance with passive DoFs unlocked, with spring and damper models used. Although no damper components were used in this system, the resistance effect of dampers was obtained by adjusting the elastic components.

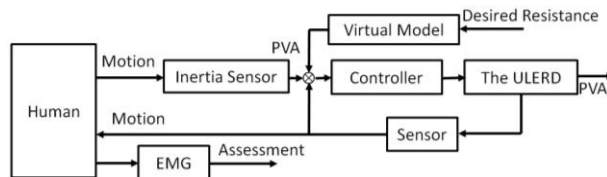


Figure 4. Control scheme for proposed system. Control strategy can be obtained in terms of the values for inertia sensor and the desired model. sEMG signals are used to assess the efficacy of proposed system.

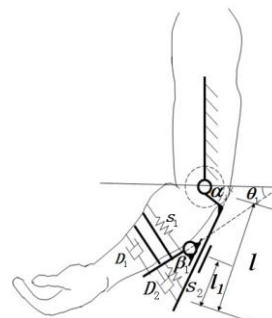


Figure 5. Schematic model of elbow resistance with passive DoFs unlocked.

3.1 Control methodology with passive DoFs unlocked

(1) Flexion motion

During flexion motion, the force exerted on the user's forearm can be calculated with respect to spring S_1 and damper D_1 using Eq. (11). Because the motor is driven using closed-loop velocity and position control, the output torque is adjusted automatically.

$$F_1 = k_1(\theta - \theta_1)l + c_1\dot{\theta} \quad (11)$$

where k_1 is the coefficient of spring s_1 ; c_1 is the coefficient of damper D_1 , which can be adjusted to match the virtual environments; θ is the angle between the user's forearm and the horizontal plane, which is detected via an inertia sensor; θ_1 is the angle between the forearm frame and the horizontal plane; $\dot{\theta}$ is the angle velocity of the user's forearm; and F_1 is the virtual resistance to the user when the user moves his or her arm. Because the damper effect is generated by adjusting elastic components, $F_1 - c\dot{\theta}$ is the actual resistance to the user and l is the length from the elastic component to the elbow axis.

The angle between the forearm frame and the horizontal plane is obtained as:

$$\theta_1 = \theta + \frac{(c_1\dot{\theta} - F_1)}{k_1l} \quad (12)$$

According to the elbow joint mechanism of the device (Fig. 5), the rotational angle of the elbow joint is obtained as:

$$\alpha - \beta = \theta_1 \quad (13)$$

where α is the angle of the elbow joint of the device and β is the angle of the passive rotational joint that can be detected by a potentiometer. The motor can be controlled based on the following equation derived from Eqs. (12) and (13):

$$\alpha = \beta + \theta + \frac{(c_1 \dot{\theta} - F_1)}{k_1 l} \quad (14)$$

Because the relative displacement of the user's forearm with respect to the frame of the device is the main factor (see Eq. (12)), traditional PID control was adapted based on closed-loop displacement.

(2) Extension motion

The force analysis during flexion motion is not the same or the reverse of that during extension motion due to the passive DoFs. During extension motion, the force exerted on the user's forearm can be calculated with respect to spring S_2 and damper D_2 using:

$$F_2 = k_2(\beta_1 - \beta)l_1 + c_2 \dot{\theta} \quad (15)$$

where β_1 is the initial angle of the passive rotated joint, l_1 is the length from the elastic component to the axis of the passive joint, c_2 is the coefficient of damper D_2 , and k_2 is the coefficient of spring S_2 .

During extension motion, the user's forearm makes contact with the frame of the device, so the following equation can be obtained:

$$\theta = \theta_1 \quad (16)$$

From Eqs. (13), (15), and (16), the following equation is obtained:

$$\alpha = \frac{(F_2 - c_2 \dot{\theta})}{k_2 l_1} - \theta - \beta_1 \quad (17)$$

where $F - c\dot{\theta}$ is the real resistance on the user's limb. The target of the control is to find the θ (or α_1) value that meets the resistance by using the closed-loop position control. Because β_1 is detected by a potentiometer that is not actuated, $\alpha - \beta_1$ is discussed as one variation in the following section.

3.2 Control methodology with passive DoFs locked

(1) Flexion motion

With considering the influence of passive DoFs on system stiffness, the passive DoFs can be locked conveniently when there is requirement of high system stiffness (Fig. 6). The force exerted on the user's forearm with respect to spring S_3 and damper D_3 is:

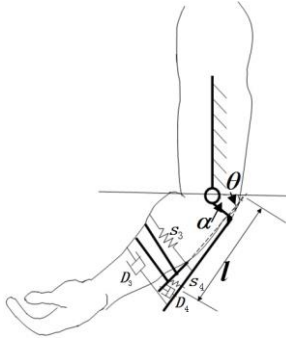


Figure 6. Schematic model of elbow resistance with passive DoFs locked.

$$F_3 = k_1(\theta - \frac{\pi}{2} + \alpha)l + c_1 \dot{\theta} \quad (18)$$

where F_3 is the desired virtual force during flexion motion with passive DoFs locked. The rotational angle of the elbow joint of the device can be obtained by rearranging Eq. (18):

$$\alpha = \frac{(F_3 - c_1 \dot{\theta})}{k_1 l} + \frac{\pi}{2} - \theta \quad (19)$$

(2) Extension motion

The force analysis during flexion motion is similar to that during extension motion:

$$F_4 = k_2(\theta - \frac{\pi}{2} + \alpha)l + c_2 \dot{\theta} \quad (20)$$

where F_4 is the virtual force during extension motion with passive DoFs locked. The rotational angle of the device elbow joint is obtained by rearranging Eq. (20):

$$\alpha = \frac{(F_4 - c_2 \dot{\theta})}{k_2 l} + \frac{\pi}{2} - \theta \quad (21)$$

4. Experiments

4.1 User interface based on virtual reality

A three-dimensional interface was created using OpenGL. Two virtual upper limbs were created in the virtual environment (Fig. 7). One was a tracked virtual arm that moves at a programmable speed within the range of motion of the user's limb, and the other was a manipulated virtual arm that showed the motion of the user's limb. The experiment required the user to manipulate the ULERD to make the manipulated virtual arm follow the tracked virtual arm from a fully extended position to extension. During this experiment, the virtual force was programmed and a certain resistance was exerted on the user.

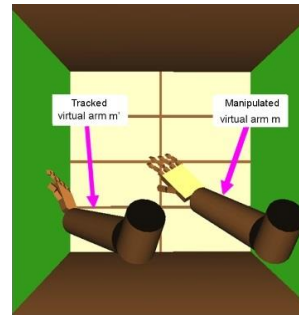


Figure 7. Virtual environment used for experiment.

4.2 sEMG signal acquisition and processing

sEMG, which is related to muscle activation, is widely used to estimate muscle torque and to drive exoskeletal devices or limb prostheses [25-31]. In this study, sEMG was adopted to detect the activation of muscles to evaluate the performance of the user's limbs during experiments. Because distinguishing muscle activation using raw sEMG signals is difficult, the sEMG data were processed.

sEMG signals from the biceps and triceps muscles were acquired to assess elbow flexion and extension. These signals were recorded using 12-mm-diameter bipolar surface electrodes located 18 mm apart at a sampling rate of 1000 Hz. Sampled data were preprocessed with a commercial sEMG acquisition and filtering device (bandwidth: 20-500 Hz) with eight channels fed to the processing program at a sampling rate of 1000 Hz (most EMG signal frequency power is contained within 20-150 Hz) through an analog-to-digital (AD) sampling board (PCI3165, Interface Co., Chiba, Japan).

Hardware and software filters were used to remove noise generated by the machine. A hardware filter was implemented via a filter box to eliminate electrical interference noise. The software filter was implemented using wavelet packet transform (WPT) via Matlab (Natick, MA, USA) because WPT has advantages compared to other filter methods and can also be used as a feature extraction tool. Daubechies 2 was selected as the mother wavelet, and the detail coefficients at the fourth decomposition level from refs. [32-34] were used to exact sEMG signal features. A statistical method was used instead of wavelet entropy. The integrated absolute value (IAV) of WPT coefficients was obtained as:

$$IAV = \sum_{n=1}^N |s_n| \quad (22)$$

where s_n is the coefficients of WPT for sEMG signals. N was set to 256.

5. Results and discussion

5.1 Experimental results

Three healthy subjects in our lab participated in the experiments, which require them to perform elbow flexion and extension wearing the ULERD. Each subject was required to perform the experiments at three levels of resistance with passive DoFs locked (C1) and unlocked (C2), respectively. In C1, the displacement of the user's forearm and the ULERD are represented in terms of $\theta - \pi/2$ and α . In C2, the displacement of the user's forearm and the forearm frame of the ULERD were are represented in terms of θ and $\alpha - \beta_1$. Each case included three levels of resistance, namely elbow flexion and extension with no resistance ($\theta - \frac{\pi}{2} - \alpha = 0$ or $\theta - \alpha + \beta_1 = 0$), low resistance ($\theta - \frac{\pi}{2} - \alpha = 3.0$ or $\theta - \alpha + \beta_1 = 3.0$), and high resistance ($\theta - \frac{\pi}{2} - \alpha = 6.0$ or $\theta - \alpha + \beta_1 = 6.0$), respectively. For each level of resistance, two sEMG signal channels from the elbow joint (e.g., biceps and triceps) of the subjects were monitored and used as performance indicators. Because of the instability of the velocity obtained via calculation, the damper coefficients c_1 and c_2 were set to 1.0 Ns/rad. Every subject performs five trials for each level.

Figure 8 shows typical results of the experiments of C1-L1 (first level with passive DoFs locked) and C2-L1 (first level with passive DoFs unlocked) from subject A. In this figure, (a1) is the motion of the user's forearm and the ULERD during C1-L1 and (b1) is the IAV of the WPT coefficients (Eq. (22)) of the sEMG signals derived from the triceps and biceps muscles.

The values at about the fourth second are higher because the forearm was moving to the horizontal plane, and the biceps were activated. In Fig. 8, (a2) shows the motion trajectories of the user's forearm and the ULERD in experiment C2-L1, and (b2) shows the IAV of the WPT coefficients for the sEMG signals derived from the triceps and biceps. The values of triceps in (b1) are almost the same as those in (b2), indicating similar triceps activation; however, values from the biceps in (b1) are lower than those in (b2), which was caused by incomplete gravity compensation by the forearm frame of the ULERD in C2.

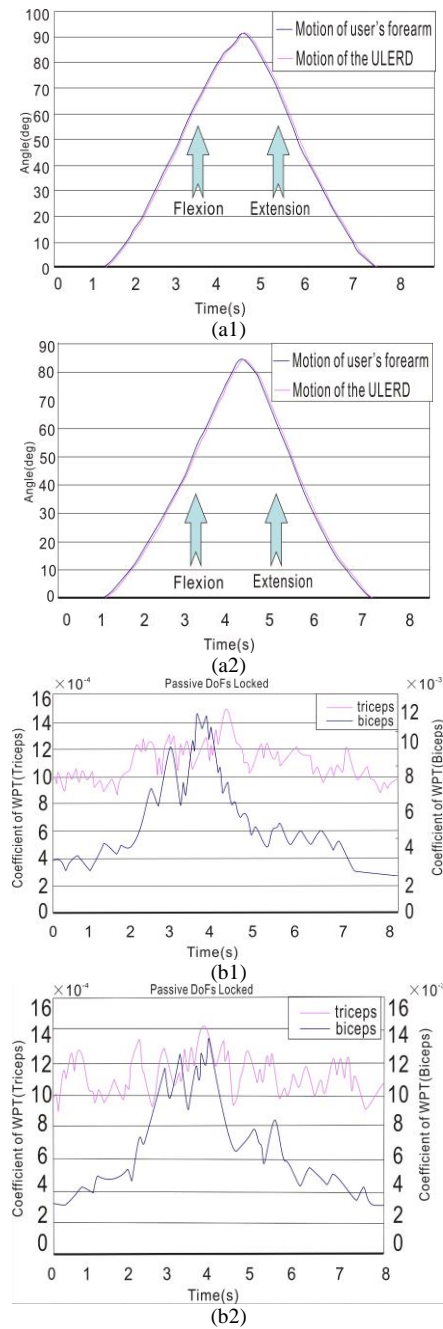


Figure 8. Typical results of experiments of C1-L1 (first level with passive DoFs locked) and C2-L1 (first level with passive DoFs unlocked) from subject A. (a1) and (b1) are the results for passive DoFs locked; (a2) and (b2) are the results for passive DoFs unlocked.

Figure 9 shows typical results of C1-L2 and C2-L2 experiments done by subject A. In this figure, low resistance was provided to the user’s forearm by setting the relative displacement between the user’s forearm and the ULERD ($\theta - \pi/2 - \alpha = 3.0$ for C1-L2 and $\theta - \alpha + \beta_1 = 3.0$ for C2-L2). In Figs. 9(a1) and (a2), there is a bulge in the motion trajectory of the ULERD because the displacement between the user’s forearm and the ULERD changed, with flexion motion changing to extension motion. In (b1), a peak appears at the fourth second, which was perhaps induced by misalignment between the user’s forearm and the ULERD. The values

derived from the biceps in (b1) are higher than those in (b2), particularly during flexion motion. In contrast, values from the triceps in (b1) are higher than those in (b2) during extension motion, indicating that the resistance exerted during C1 was higher than that during C2, because the structure with passive DoFs locked is stiffer than that with passive DoFs unlocked. However, the resistance provided in C2 was smoother than that provided in C1 because the misalignment was corrected.

Figure 10 shows typical results of C1-L3 and C2-L3 experiments of subject A. In this figure, high resistance was provided to the user’s forearm by setting the relative

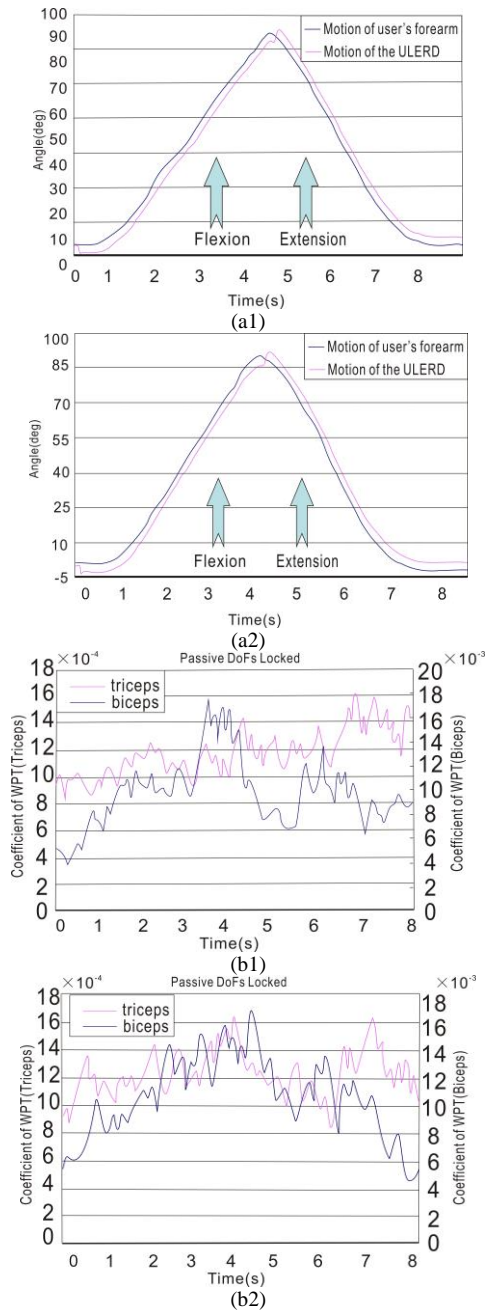


Figure 9. Typical results of experiments of C1-L2 (second level with passive DoFs locked) and C2-L2 (second level with passive DoFs unlocked) from subject A. (a1) and (b1) are the results for passive DoFs locked; (a2) and (b2) are the results for passive DoFs unlocked.

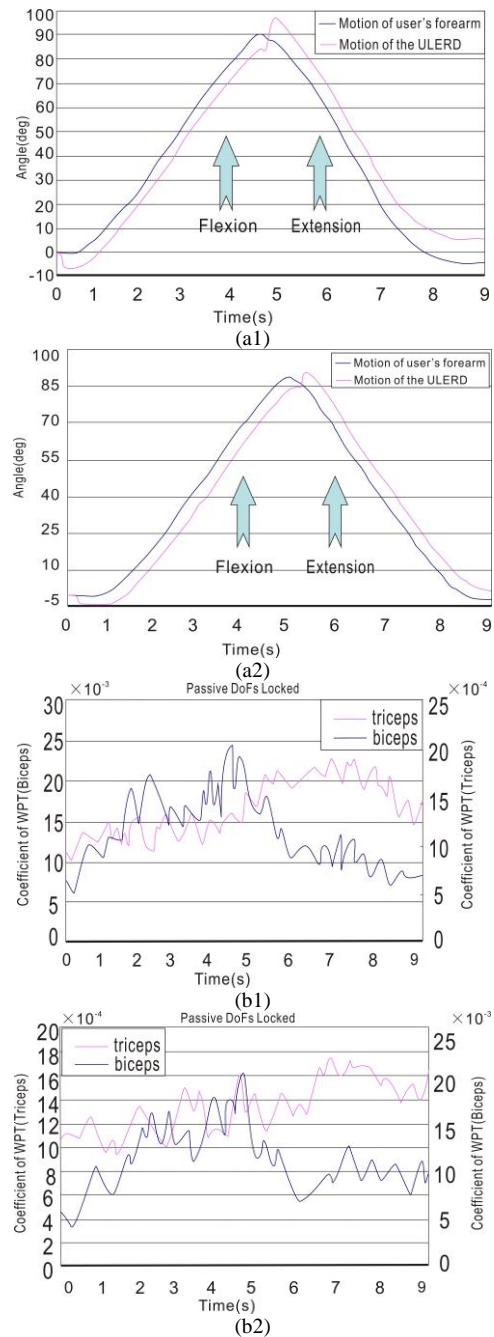


Figure 10. Typical results of experiments of C1-L3 (third level with passive DoFs locked) and C2-L3 (third level with passive DoFs unlocked) from subject A. (a1) and (b1) are the results for passive DoFs locked; (a2) and (b2) are the results for passive DoFs unlocked.

displacement between the user's forearm and the ULERD ($\theta - \pi/2 - \alpha = 6.0$ in C1-L3 and $\theta - \alpha + \beta_1 = 6.0$ in C2-L3). Similar to the previous figures, the values from the biceps during flexion increased and then decreased during extension motion in (b1) and (b2). However, the results from the triceps are opposite to those from the biceps. According to (b1) and (b2). The values from the biceps and triceps in (b1) are higher than those in (b2), which indicates that the stiffness of structure with passive DoFs locked is higher than that of the structure with passive DoFs unlocked.

Table 2 shows the mean values of IAV (Eq.22) obtained by processing the biceps and triceps sEMG signals in the three C1 and C2 experiments for subjects A, B, and C. Because the activation of the biceps and triceps muscles is different during elbow flexion and extension, the mean values of IAV for flexion and extension were calculated separately. The value of the biceps during flexion during C1-L1 is lower than that during C2-L1 because the gravity of the ULERD forearm frame was not completely compensated. The biceps flexion value during C1-L2 is higher than that during C1-L1, indicating that the low resistance provided to the user was effective. The biceps flexion value during C1-L3 is higher than that during C1-L2, indicating that the high resistance provided to the user was effective. The biceps value during C1-L3 is higher than that during C2-L3, which indicates the stiffness of the structure with passive DoFs locked was higher than that with passive DoFs unlocked. Similar results were obtained during extension. The activation of the triceps is higher in L3 than in L1 and L2. The passive DoFs decreased the activation of the triceps muscle during extension in L2 and L3.

Table 2. Mean IAV values of sEMG signals for C1 and C2 experiments for three subjects ($\times 10^{-3}$) (F: flexion; E: extension; B: biceps; T: triceps).

Subject		A		B		C				
		C1	C2	C1	C2	C1	C2			
Experiment	L1	F	B	5.83	7.31	4.48	6.14	7.28	9.16	
		T	B	1.12	1.25	0.91	1.18	1.24	1.46	
	E	B	B	4.07	4.15	3.44	3.19	4.99	5.35	
		T	B	1.02	1.31	1.15	0.99	1.31	1.67	
	L2	F	B	B	10.4	10.7	8.79	9.07	11.9	10.2
			T	B	0.97	1.30	0.87	1.13	1.26	1.49
E		B	B	9.33	9.51	6.94	6.61	10.8	11.5	
		T	B	1.81	1.59	1.77	1.71	2.29	2.41	
L3	F	B	B	15.8	12.7	14.1	13.3	21.1	18.8	
		T	B	1.24	1.19	0.89	1.22	1.45	1.57	
	E	B	B	11.2	9.86	7.54	8.11	12.9	12.3	
		t	B	2.57	1.91	2.71	2.23	3.17	2.80	

5.2 Discussion

Different from other rehabilitation robots, the ULERD is designed to be portable and wearable, and it can be supported by the user. It induces a complex contact condition between the robot and the user, so that the contact force is not able to be detected accurately using force sensors. To implement resistance training, based on traditional impedance and admittance control, user motion is detected rather than device motion. Elastic components are used to create the physical elastic relationship between the user and the device. The desired impedance applied

to the subject can be generated by combining the motion the subject and the elastic models.

In the proposed device, passive DoFs, which can be locked or unlocked, were designed to correct the misalignment between the device and the human body. Two sets of experiments were conducted to evaluate the proposed method during resistance training, namely one set with passive DoFs unlocked and one set with passive DoFs locked. Passive DoFs make it more comfortable for users to perform passive training motion wearing the ULERD; however, they reduced the stiffness of the entire mechanical structure, so the effect of resistance training was not as good as that with passive DoFs locked.

SEMG signals describing muscle activity were used to evaluate the proposed method and to generate resistance to the human forearm using the ULERD. The relationship between the torques exerted from muscles and sEMG signals was not discussed because many studies have reported on it. The effects of the proposed method implemented during elbow flexion and extension were obtained by processing the sEMG signals derived from the biceps and triceps muscles. The accuracy of the proposed method depends on the device structure.

6. Conclusion

An upper-limb exoskeleton rehabilitation device was proposed and developed for home rehabilitation. Due to the lack of backdrivability and accurate detection of the contact force between the human and the device, a method that detects the motion of the human forearm instead of the device was proposed and implemented with passive DoFs locked and unlocked, respectively. The structure of the passive DoFs was designed to correct misalignment between the human and the device to allow more user comfort; however, it reduced the device stiffness so that resistance training could not be implemented completely according to the experimental results, particularly with high resistance. Experimental results indicate that the proposed method of exerting resistance can be implemented with passive DoFs locked and unlocked, respectively, with the latter showing higher stiffness and higher resistance. The proposed method is effective for use with the ULERD and will be further tested for home rehabilitation in future work.

Acknowledgement

This research was supported by the Kagawa University Characteristic Prior Research Fund 2012.

References

- [1] G. Thielman and P. Bonsall, "Rehabilitation of the upper extremity after stroke: a case series evaluating REO therapy and an auditory sensor feedback for trunk control," *Stroke Res. Treat.*, 2012: 348631, 2012.
- [2] Langhorne P, Coupar F and Pollock A., "Motor recovery after stroke: A systematic review," *Lancet Neurol.*, 8: 741-754, 2009.
- [3] Paul L., Debbie H., Jennifer B., Hervé L., Don G, Jacob A. and Alex M., "A haptic-robotic platform for upper-limb reaching stroke therapy: Preliminary design and evaluation results," *J. Neuroeng. Rehabil.*, 5: 15, 2008.

- [4] N. S. Christopher, B. G. Sasha, J. H. Rahsaan and S. L. Peter, "Development and pilot testing of HEXORR: Hand EXOskeleton rehabilitation robot," *J. Neuroeng. Rehabil.*, 7: 36, 2010.
- [5] K. Kazuo, H. R. Mohammad and S. K. T. Makoto, "Development of a 3DOF mobile exoskeleton robot for human upper-limb motion assist," *Robot. Auton.Syst.*, 56: 678-691, 2008.
- [6] W. Wang, B. Tsai, L. Hsu, L. Fu and J. Lai, "Guidance control-based exoskeleton rehabilitation robot for the upper limb", *J. Med. Biol. Eng.*, doi:10.5405/jmbe.1663, Feb 5, 2014.
- [7] A. U. Pehlivan, O. Celik and M. K. O'Malley, "Mechanical design of a distal arm exoskeleton for stroke and spinal cord injury rehabilitation," *2011 IEEE Int. Conf. on Rehabil. Robotics*, 633-637, 2011.
- [8] J. Mehrholz and M. Pohl, "Electromechanical-assisted gait training after stroke: a systematic review comparing end-effector and exoskeleton devices," *J. Rehabil. Med.*, 44: 193-199, 2012.
- [9] J. A. Kleim, E. Lussnig, E. R. Schwarz, T. A. Comery and W. T. Greenough, "Synaptogenesis and FOS expression in the motor cortex of the adult rat after motor skill learning," *J. Neurosci.*, 16: 4529-4535, 1996.
- [10] R. J. Nudo, "Adaptive plasticity in motor cortex: Implications for rehabilitation after brain injury," *J. Rehabil. Med.*, 41: 7-10, 2003.
- [11] L. G. Cohen and M. Hallett, "Neural plasticity and recovery of function," In: *Greenwood RJ, Barnes MP, McMillan TM, Ward, CD. Handbook of Neurological Rehabilitation*, 99-111, 2003.
- [12] E. Taub, G. Uswatte and R. Pidikiti, "Constraint-induced movement therapy: A new family of techniques with broad application to physical rehabilitation-A clinical review," *J. Rehabil. Res. Dev.*, 36: 237-251, 1999.
- [13] S. Guo and Z. Song, "A novel motor function training assisted system for upper limbs rehabilitation," *Proc. of IEEE Int. Conf. on Intell. Robot and Syst.*, 1025-1030, 2009.
- [14] Z. Song, S. Guo and Y. Fu, "Development of an upper extremity motor function rehabilitation system and an assessment system," *Int. J. Mechatron. Autom.*, 1: 19-28, 2011.
- [15] Z. Song and S. Guo, "Implementation of self-rehabilitation for upper limb based on a haptic device and an exoskeleton device," *Proc. of IEEE Int. Conf. on Mechatron. and Autom.*, 1911-1916, 2011.
- [16] Z. Song and S. Guo, "Design process of a novel exoskeleton rehabilitation device and implementation of bilateral upper limb motor movement," *J. Med. Biol. Eng.*, 32: 323-330, 2012.
- [17] R. Q. van der Linde, P. Lammertse, E. Frederiksen and B. Ruiter, "The HapticMaster, a new high-performance haptic interface," *Proc. Eurohaptics 2002*, 8-10, 2002.
- [18] Z. Song, S. Guo, N. Xiao, B. Gao and L. Shi, "Implementation of human-machine synchronization control for active rehabilitation using an inertia sensor," *Sensors*, 12: 16046-16059, 2012.
- [19] D. W. Robinson, J. Pratt, D. Paluska and G. Pratt, "Series elastic actuator development for a biomimetic walking robot," *Proc. of IEEE/ASME Int. Conf. on Advanced Intell. Mechatron.*, 561-568, 1999.
- [20] Masiero S, Rosati G, Valarini S and Rossi A, "Post-stroke robotic training of the upper limb in the early rehabilitation phase" *Funct Neurol.*, 24: 203-206, 2009.
- [21] H. G. Malabet, R. A. Robles and K. B. Reed, "Symmetric motions for bimanual rehabilitation," *IEEE/RSJ Int. Conf. on Intell. Robot and Syst.*, 5133-5138, 2010.
- [22] A. Ericson, A. Stark and A. Arndt, "Variation in the position of the elbow flexion axis after total joint replacement with three different prostheses," *J. Shoulder Elbow Surg.*, 17: 760-767, 2008.
- [23] Y. Ren, H. S. Park, Y. Li, L. Wang and L. Zhang, "A wearable robot for upper limb rehabilitation of patients with neurological disorders," *IEEE Int. Conf. on Robot on Biomim.*, 64-68, 2010.
- [24] C. Butefisch, H. Hummelsheim, P. Denzler and K. H. Mauritz, "Repetitive training of isolated movements improves the outcome of motor rehabilitation of the centrally paretic hand," *J. Neurol. Sci.*, 130: 59-68, 1995.
- [25] E. A. Clancy and N. Hogan, "Relating agonist-antagonist electromyograms to joint torque during isometric, quasi-isotonic, nonfatiguing contractions," *IEEE Trans. on Biomed. Eng.*, 44: 1024-1028, 1997.
- [26] A. D. Skyler, A. V. Huseyin and G. Michael, "A Method for the control of multigrasp myoelectric prosthetic hands," *IEEE Trans. Neural Syst. Rehabil. Eng.*, 20: 58-67, 2012.
- [27] K. Ullah1, A. Khan1, Ihtesham-ul-Islam1 and Mohammad A. U. Khan, "Electromyographic (EMG) signal to joint torque processing and effect of various factors on EMG to torque model," *J. Eng. Technol. Res.*, 3: 330-341, 2011.
- [28] W. L. Sang, M. W. Kristin, A. L. Blair and G. K. Derek, "Subject-specific myoelectric pattern classification of functional hand movements for stroke survivors," *IEEE Trans. Neural. Syst. Rehabil. Eng.*, 19: 558-566, 2011.
- [29] B. Elizabeth, Brokaw, Iian Black, Rahsaan J. Holley and Peter S. Lum, "Hand spring operated movement enhancer (HANDSOME): a portable, passive hand exoskeleton for stroke rehabilitation," *IEEE Trans. Neural. Syst. Rehabil. Eng.*, 19: 391-399, 2011.
- [30] F. Anders, S. Erik, AdrianD. C.Chan, E. Kevin and S. Øyvind, "Resolving the limb position effect in myoelectric pattern recognition," *IEEE Trans. Neural. Syst. Rehabil. Eng.*, 19: 644-651, 2011.
- [31] A. D. Skyler, A. V. Huseyin and G. Michael, "A Method for the control of multigrasp myoelectric prosthetic hands," *IEEE Trans. Neural. Syst. Rehabil. Eng.*, 20: 58-67, 2012.
- [32] M. W. Jiang, R. C. Wang, J. Z. Wang and D. W. Jin, "A method of recognizing finger motion using wavelet transform of surface emg signal," *Conf. Proc. IEEE Eng. Med. Biol. Soc.*, 3: 2672-2674, 2005.
- [33] M. Weeks, "Digital signal processing using MATLAB and wavelets," *Jones and Bartlett Publishers*, 2011.
- [34] G. Saevarsson, J. R. Sveinsson and J. A. Benediktsson, "Wavelet-package transformation as a preprocessor of EEG waveforms for classification," *Proc. of 19th Int. Conf. IEEE on Eng. Med. Biol. Soc.*, 3: 1305-1308, 1997.